J Biol Phys (2007) 33:271–290
DOI 10.1007/s10867-008-9066-3

ORIGINAL PAPER

Recurring Plankton Bloom Dynamics Modeled via Toxin-Producing Phytoplankton

Subhendu Chakraborty · Samrat Chatterjee · Ezio Venturino · J. Chattopadhyay

Received: 15 November 2006 / Accepted: 18 May 2007 / Published online: 11 June 2008

Abstract A simple nutrient–phytoplankton model is proposed and analyzed in the presence of toxic chemicals released by toxin-producing phytoplankton (TPP) to understand the dynamics of seasonally recurring bloom phenomena. We observe that the presence of toxic chemicals helps to explain the bloom phenomenon. We have further studied our proposed system by varying the toxin liberation rate. Our model displays a wide range of dynamical behaviours, from simple cyclical blooms to irregular chaotic blooms. We also observe skipping phenomenon. The effect of toxic chemicals released by TPP cannot, thus, be ignored in 'bottom-up' models.

Keywords Toxin-producing phytoplankton · Nutrient · Seasonal bloom · Chaos

1 Introduction

Plankton is the basis of all aquatic food chains, and phytoplankton in particular lies on the first trophic level of the food chain. Plankton dynamics is a fascinating and interesting subject of research. The mechanism for bloom formation and its possible control are

J. Chattopadhyay is supported by the Ministry of Foreign Affairs Indo-Italian program of cooperation in Science and Technology, "Biomedical Sciences". S. Chatterjee is supported by *Ministero dell'Istruzione, dell'Università e della Ricerca, Bando per borse a favore di giovani ricercatori indiani*. S. Chakraborty is supported by the Council of Scientific and Industrial Research, Human Resource Development Group, New Delhi.

S. Chakraborty · J. Chattopadhyay (✉)
Agricultural and Ecological Research Unit, Indian Statistical Institute,
203, B. T. Road Kolkata 700108, India
e-mail: joydev@isical.ac.in

S. Chatterjee · E. Venturino
Dipartimento di Matematica, Università di Torino, via Carlo Alberto 10, 10123 Turin, Italy

not yet well established. Special attention toward these issues is required from both the theoretical and the experimental points of view. Hay and Kubanek [1] pointed out that approximately 7% of phytoplankton species are responsible for bloom formation. The adverse effects of blooms on human health, recreational fisheries, tourism, the environment and ecosystems are well known [2]. To understand the fascinating dynamics of bloom formation and termination, 'top-down' mechanism [3–9], 'bottom-up' mechanism [10–15] and the simultaneous effect of top-down and bottom-up mechanisms [16–22] have been proposed and analyzed.

The ecological role of algal toxins is of great importance and cannot be ignored. It is well known that some phytoplankton species have the ability to release toxic or allelochemicals into the environment which are harmful to other algal species [23]. Various experimental results suggest that optimal requirements of environmental conditions, environmental stress factors, nutrient-limited conditions, etc., are the main factors for toxin liberation (e.g. see [24–27]. Chattopadhyay and his co-workers, with the help of field observations and mathematical models, have established that toxin-producing phytoplankton (TPP) acts as a controlling agent for the termination of plankton blooms [16, 21]. Graneli and Johansson [28] performed a laboratory experiment to observe the effects of prymnesium toxins on the growth of *Thalassiosira weissflogii*, *Rhodomonas* cf. *baltica* and *Prorocentrum minimum*. They concluded that the decrease in cell concentration of each of the three tested species is not due to nutrient limitations but is mainly caused by the amount of toxin released by the species. The above findings motivate us to study the effect of TPP on bottom-up models.

To the best of our knowledge, Huppert et al. [11] are the pioneers who studied the bloom dynamics of phytoplankton using the bottom-up approach. The main motivation of the present work is to observe the role of TPP on bottom-up models. For better understanding of such a situation, we present a brief overview of the works of Huppert et al. [11, 13].

In Huppert et al. [11], the following N-P model is considered:

$$\left.\begin{aligned} \frac{dN}{dt} &= a - bNP - eN, \\ \frac{dP}{dt} &= \quad cNP - dP. \end{aligned}\right\} \tag{1}$$

Here, N (g m^{-3}) is the nutrient level and P (mg m^{-3}) is the phytoplankton population. The non-negative parameters are interpreted as follows:

- a Constant external nutrient inflow
- b Maximal nutrient uptake rate of phytoplankton
- c Maximal conversion rate of nutrient into phytoplankton
- d Per capita-mortality rate of phytoplankton
- e Per capita-loss rate of nutrients

The mechanism of bloom formation and the cause of its termination are described by the above model using phase plane analysis. They divided the whole phase space into three stages. Their investigation showed that, due to constant nutrient input, the level of nutrients gradually increases initially (linear nutrient build up; stage 1); in the subsequent stage, they observed the rapid growth of phytoplankton, resulting in the bloom; in this stage, the nutrient concentration also reaches its maximum value (rapid growth of P and nutrient concentration; stage 2). In the final stage, both nutrient concentration and phytoplankton bloom crash because the phytoplankton growth attains its maximum value and rapidly

exhausts the available nutrient concentration (rapid decline of N and P; stage 3). However, according to them, a phytoplankton bloom is not necessarily a single event; sometimes, the major bloom is succeeded by a number of smaller secondary blooms. They have also observed the effect of different initial values of the phytoplankton population on the bloom height P_{max}. They found that, for a small initial phytoplankton population P_0 (specifically, below the N nullcline), the final amount of accumulated nutrients, N_{max}, becomes large and then causes a larger P_{max} value. However, for larger values of P_0 (i.e. above the N nullcline), the reverse phenomenon is observed; a bigger bloom corresponds to a larger P_0 value. However, the role of initial nutrient level in bloom formation is not clear here. Also, this generic NP model is unable to represent the periodic cycles and the skipping phenomena for blooms, which are common in nature.

To overcome this situation, Huppert et al. [13] extended their basic NP model (1) by introducing periodic seasonal forcing on phytoplankton growth. They considered the growth of phytoplankton as a step function

$$\beta(t) = \begin{cases} \beta^+ = 1+\delta, & \textit{High season}. \\ \beta^- = 1-\delta, & \textit{Low season}, \end{cases} \tag{2}$$

where δ controls the strength of the seasonal forcing and the time scale is such that there are two equally long seasons per time period $\tau = \frac{2\pi}{\omega}$.

With this assumption, model (1) becomes

$$\left.\begin{aligned} \frac{dN}{dt} &= a - b\beta(t)NP - eN, \\ \frac{dP}{dt} &= c\beta(t)NP - dP. \end{aligned}\right\} \tag{3}$$

Their investigations showed that (2) leads to all sorts of complex dynamics, including limit cycles, chaos, skipping phenomena, etc.

2 A Simple Nutrient–Phytoplankton Model with Toxic Effect

Interactions between phytoplankton species due to excretion of extracellular organic substances is an important factor for phytoplankton succession [29]. Keating [30] reported that toxic substances from cyanobacteria inhibit the growth of diatoms. Schmidt and Hansen [31] also found that *Chyrsochromulina polylepis* had a strong allelopathic effect on the dinoflagellate *Heterocapsa triquetra*. Similarly, some flagellate and dinoflagellate species have been found to secrete substances inhibiting those microalgae that do not produce toxins [32]. The above experimental observations clearly demonstrate that the extra mortality of non-toxic phytoplankton is due to toxin. We assume that the rate of toxin release by the TPP is proportional to the crowding of the phytoplankton and, for low values of the population, this should be expressed by a P^2 term, and then it increases to a maximal value when the phytoplankton population tends toward large values. This is because, for low values of the phytoplankton population, the toxin release is low anyway, and also, its killing rate must be low as well because, for low densities, phytoplankton may well escape the poison effects. For large values of the population, the toxin release has, in any case, a maximal biological limit. Thus, the Holling type III functional form is the best suited to model this effect. We then consider the Holling type III functional form to represent the extra mortality of phytoplankton due to the release of toxic chemicals.

With the above assumptions, the system (1) becomes

$$\left.\begin{aligned} \frac{dN}{dt} &= a - bNP - eN, \\ \frac{dP}{dt} &= cNP - dP - \frac{\theta P^2}{\mu^2 + P^2}. \end{aligned}\right\} \tag{4}$$

Here, θ (g $(m^3$ $year)^{-1}$) represents the rate of release of toxic chemicals by the TPP population and μ denotes the half-saturation constant. Note that, in the absence of the toxic effects, system (4) reduces to system (1). The other parameters bear the same meaning as described in system (1). System (4) is to be analyzed with initial conditions $N(0) = N_0 > 0$ and $P(0) = P_0 > 0$.

2.1 Positive Invariance

Let us put (4) in a vector form by setting $X = (N,\ P)^T \in R^2$, so that we have

$$F(X) = \begin{bmatrix} F_1(X) \\ F_2(X) \end{bmatrix} = \begin{bmatrix} a - bNP - eN \\ cNP - dP - \dfrac{\theta_1 P^2}{\mu^2 + P^2} \end{bmatrix} \tag{5}$$

where $F : C_+ \to R^2$ and $F \in C^\infty(R^2)$. Then, (4) becomes

$$\dot{X} = F(X) \tag{6}$$

with $X(0) = X_0 \in {R_+}^2$. It is easy to check in (5) that, whenever choosing $X(0) \in {R_+}^2$ such that $X_i = 0$, then $F_i(x)\,|_{X_i=0} \geq 0$, $(i = 1, 2)$. Now, any solution of (6) with $X_0 \in {R_+}^2$, say $X(t) = X(t; X_0)$, is such that $X(t) \in {R_+}^2$ for all $t > 0$ [33].

2.2 Boundedness of the System

Theorem 1 *All the solutions of* (4) *are ultimately bounded.*

Proof We define a function

$$w = N + P. \tag{7}$$

Because $c \leq b$, the time derivative of (7) along the solutions of (4) is given by

$$\begin{aligned} \frac{dw}{dt} &= a - (b - c)NP - eN - dP - \frac{\theta_1 P^2}{\mu^2 + P^2} \\ &\leq a - eN - dP. \end{aligned}$$

Taking $\zeta > 0$, we obtain

$$\frac{dw}{dt} \leq a + (\zeta - e)N + (\zeta - d)P.$$

Now, if we choose $\zeta \leq \min(e, d)$

$$\frac{dw}{dt} + \zeta w \leq A.$$

Applying these results of differential inequalities, we obtain

$$0 < w(N, P) < \frac{a}{\zeta}\left(1 - e^{-\zeta t}\right) + w(N(0), P(0))e^{-\zeta t}.$$

For $t \to \infty$, we have $0 < w < \frac{a}{\zeta}$. Hence, all solutions $(N(t), P(t))$ of (4) that initiate at $(N(0), P(0)) \in \mathbb{R}^2_{0,+}$, are confined in the region

$$G = \left((N, P) \in \mathbb{R}^2_{0,+} : \ w = \frac{a}{\zeta} + \epsilon, \ \textit{for any} \ \epsilon > 0 \right),$$

for all $t \geq T$, where T depends on the initial values $(N(0), P(0))$. Thus, the set G is an invariant set which contains the Ω-limit set of all the paths of system (4) that initiate in the positive octant. □

2.3 Equilibrium Points and their Stability

The equilibrium points are $E_1\left(\frac{A}{e}, 0\right)$ and $E^*(N^*, P^*)$, where

$$N^* = \frac{a}{e + bP^*},$$

and P^* is a root of the equation

$$bdP^3 + (b\theta_1 - (ac - de))P^2 + \left(\theta_1 e + bd\mu^2\right)P - (ac - de)\mu^2 = 0. \tag{8}$$

It is clear from (8) that

1. If $ac - de \leq 0$, (8) has no positive solutions.
2. If $0 < ac - de \leq b\theta_1$, (8) has a unique positive solution.
3. If $b\theta_1 < ac - de$, then (8) has either three or one positive solutions

The dynamical behaviour of system (4) about E_1 and E^* is stated in the following two lemmas. The proof is obvious and, hence, omitted.

Lemma 1 *The equilibrium point E_1 of system (4) is locally asymptotically stable if $ac - de < 0$.*

Lemma 2 *The equilibrium point E^* of system (4) is locally asymptotically stable if*

$$bP^* + e - + d + \frac{ac}{bP^* + e} + \frac{2\mu^2\theta P^*}{\mu^2 + P^{*2}} > 0.$$

2.4 Numerical Experiments

Numerical experiments of the nutrient–phytoplankton dynamics using Matlab 7.1 are presented in Fig. 1. To observe the dynamics of system (4), we have varied the parameter θ, keeping the other parameter values fixed. The set of fixed parameter values are taken from various literature sources and are given in Table 1.

Figure 1a depicts the dynamics of system (4) with $\theta = 0$; the same figure was also drawn by Huppert et al. [11]. Their observations are described in Section 1. However, it is interesting to note that the dynamics observed by Huppert et al. [11] are true only for $\theta \leq \theta_c \equiv 0.05$. As we mentioned earlier, the role of toxic chemicals cannot be ignored.

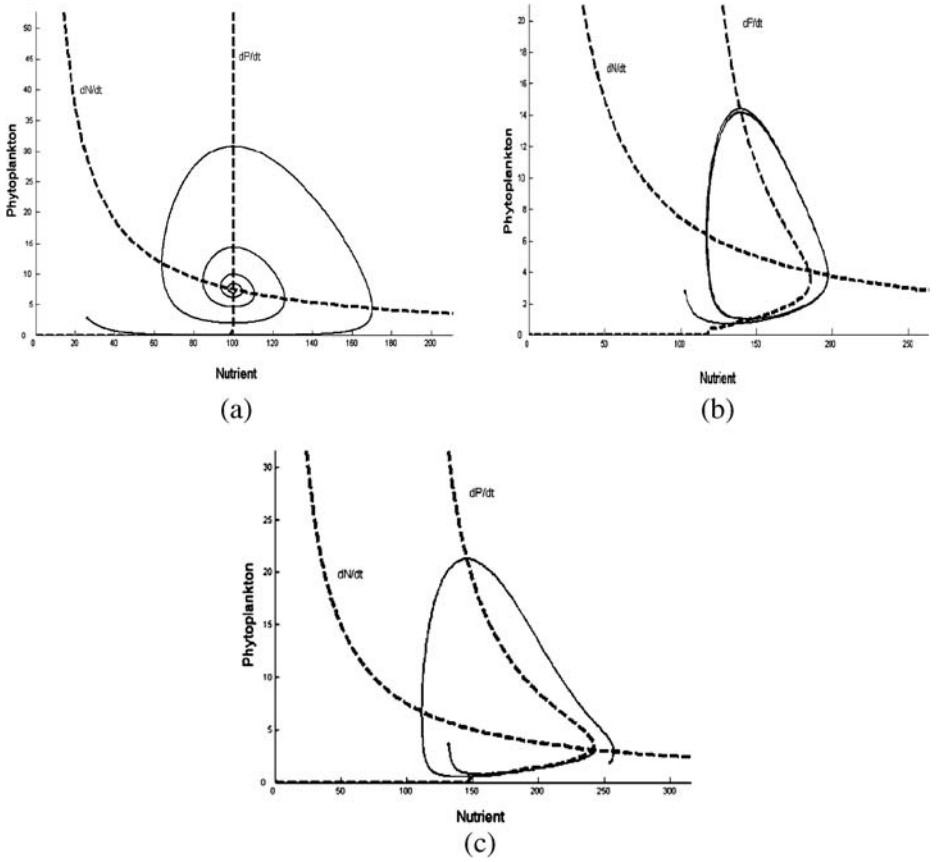

Fig. 1 **a** Phase plane diagram of the phytoplankton bloom (compare Fig. 3b in Huppert et al. [11]) of system (4) with $\theta = 0$. **b** Phase plane diagram of the nutrient–phytoplankton dynamics of system (4) with $\theta = 0.06$. **c** Phase plane diagram of the nutrient–phytoplankton dynamics of system (4) with $\theta = 0.1$

Turner and Tester [34] observed that phycotoxins vary in their modes of action, levels of toxicity and solubility. Keeping their experimental observation in mind, we have changed the value of θ. For example, if we take the value of $\theta = 0.06$, the spiral sink shown in Fig. 1a modifies to a limit cycle behaviour (see Fig. 1b). If we further increase the value of θ to 0.1, the equilibrium point changes to a nodal sink (see Fig. 1c).

Now, we summarise the above findings:

1. From Fig. 1a, we observe that, for a certain critical value of θ ($\theta \leq 0.05$), the mechanism of bloom formation and its termination can be explained and is already elaborately described by Huppert et al. [11] for $\theta = 0$.
2. In reality, the occurrence of bloom is periodic. Figure 1b clearly depicts this phenomenon for $\theta = 0.06$. All three stages (stage 1–stage 3, described in Section 1) are observed here, but the most interesting point is that, when the phytoplankton population is very low, there is an increase in the nutrient concentration and the whole process is repeated again, resulting in another bloom.

Table 1 The set of fixed parameter values taken from various literature sources

Parameter	Definition	Values	Reference
a	Constant nutrient input flow	0.00075 mg $(m^3\ year)^{-1}$	Huppert et al. [11]
b	Nutrient uptake rate of phytoplankton	1.0 $m^3\ (g\ year)^{-1}$	Huppert et al. [11]
c	Nutrient conversion rate of phytoplankton	1.0 $m^3\ (mg\ year)^{-1}$	Huppert et al. [11]
d	Per capita-mortality rate of phytoplankton	0.1 $year^{-1}$	Huppert et al. [11]
e	Per capita-loss rate of nutrient	0.0 $year^{-1}$	Huppert et al. [11]
μ	Half saturation constant	0.035 g m^{-3}	Edward and Brindley [5]

3. Finally, when the value of θ increases to 0.1, we observe that the presence of toxin helps to control the bloom. From the phase plane diagram shown in Fig. 1c, the solution curve moves directly to the coexisting equilibrium point, preventing bloom occurrence. For the reoccurrence of bloom, a sufficiently high level of initial nutrients is needed. Thus, the level of toxicity plays an important role in the recurring plankton blooms. This observation supports the experimental findings of Turner and Tester [34].

It is interesting to observe the dynamics of bloom heights for the system (4) with different initial phytoplankton populations. We observe that, when the initial phytoplankton level P_0 is below the N nullcline, a relatively smaller P_0 gives the maximum bloom height. The reverse dynamics is observed when P_0 is above the N nullcline. (Figures are not shown as these are similar to Fig. 7b of Huppert et al. [11].)

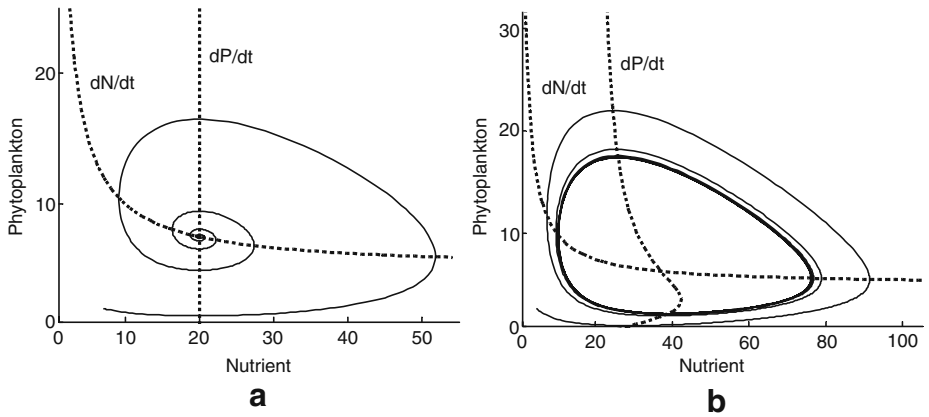

Fig. 2 **a** Phase plane diagram of the nutrient–phytoplankton dynamics of the equation (9) with $\theta = 0.0$. **b** Phase plane diagram of the nutrient–phytoplankton dynamics of system (9) with $\theta = 0.015$

Can we observe the same dynamics of system (4) if we replace the simple multiplicative resource uptake by a more realistic saturating functional response, e.g. Holling type II? With this assumption, system (4) becomes

$$\left.\begin{aligned} \frac{dN}{dt} &= a - \frac{bNP}{\gamma + N} - eN, \\ \frac{dP}{dt} &= \frac{cNP}{\gamma + N} - dP - \frac{\theta P^2}{\mu^2 + P^2}. \end{aligned}\right\} \tag{9}$$

With the same parameter set of values as in Table 1, and for $\gamma = 0.1$ (which is within the reported range of Edwards and Brindley [5]) and $b = c = 1.5$, we obtain Fig. 2a for $\theta = 0$ and Fig. 2b for $\theta = 0.015$. Thus, the above observations indicate that reoccurrence of phytoplankton bloom also holds if the simple multiplicative resource uptake is replaced by Holling type II.

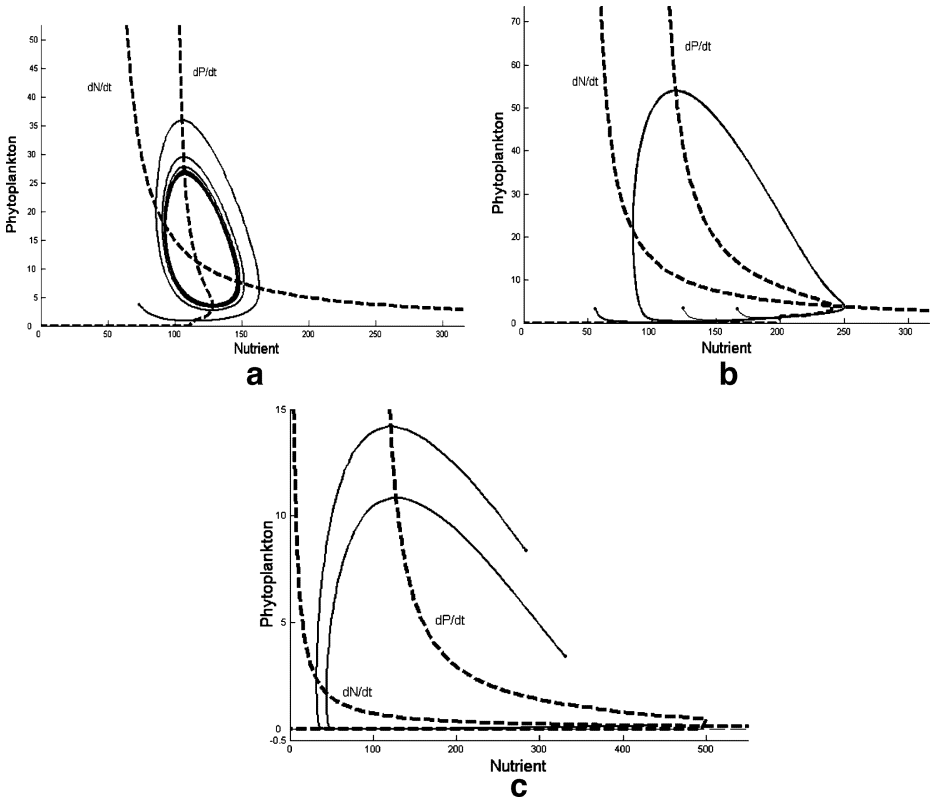

Fig. 3 Phase plane diagram of the nutrient–phytoplankton dynamics given in the equation (10) in the presence of nutrient recycling, with $k = 0.05$, for **a** $\theta = 0.02$, **b** $\theta = 0.1$, and **c** $\theta = 0.3$

In nature, the dead phytoplankton enhance the nutrient concentration. System (4) has then been modified further by taking into account the recycling factor. If we denote by $k < d$ the portion of the phytoplankton recycled back to the nutrient concentration, we obtain

$$\left.\begin{aligned} \frac{dN}{dt} &= a - bNP - eN + kP, \\ \frac{dP}{dt} &= cNP - dP - \frac{\theta P^2}{\mu^2 + P^2}. \end{aligned}\right\} \tag{10}$$

Numerical simulations have been performed with the same set of parameter values as in Table 1 and for $k = 0.05$. Our findings as a function of θ are summarised in Fig. 3.

The limit cycle behaviour indicating recurring blooms is obtained in the range $0.02 \leq \theta \leq 0.2$ (Fig. 3a and b). When the value of θ crosses 0.2, the equilibrium becomes a node; see Fig. 3c.

Thus, inclusion of nutrient recycling enhances the chances of recurring bloom dynamics. To control such a bloom, a higher concentration of toxic chemicals would be needed.

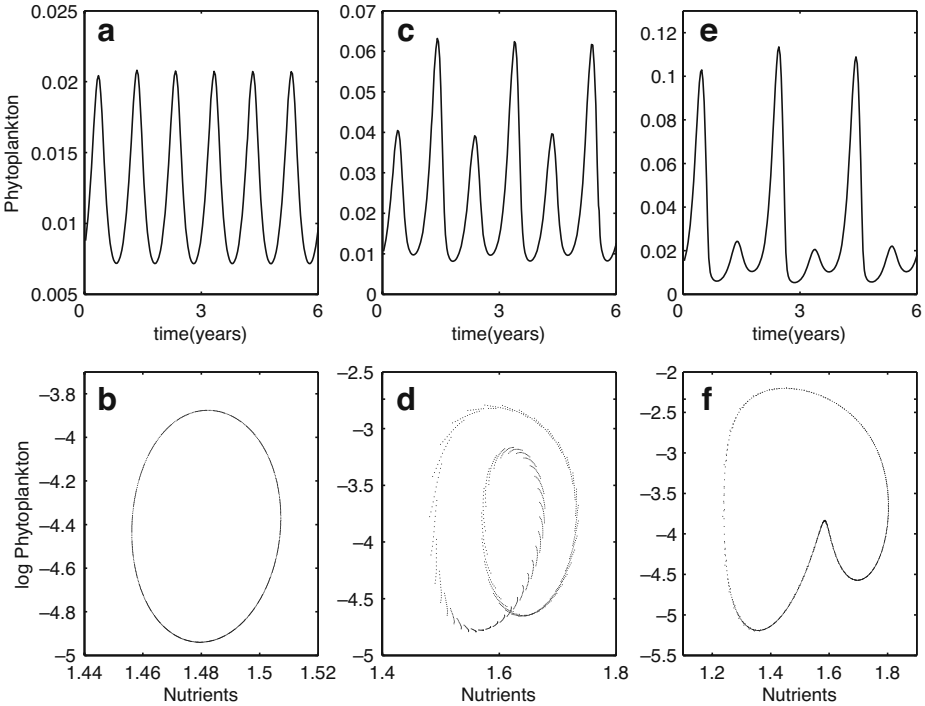

Fig. 4 Periodic solutions of model equations (11) for different parameters. *Top panel*: Time-series. *Bottom panel*: Phase plane. **a**, **b** $a = 0.02$; **c**, **d** $a = 0.04$; **e**, **f** $a = 0.045$. Fixed parameters: $b = 1$; $c = 1$; $d = 1$; $e = 0.0012$; $\omega = 0.19$; $\delta = 0.5$; $\mu = 0.35$; $\lambda = 0.06$

3 Nutrient–Phytoplankton Model with Periodicity in Toxic Chemicals

The model proposed by Huppert et al. [13] shows the bloom's skipping dynamics, which is generally seen in real data sets. In their opinion, the skip generally occurs due to the seasonal changes, which implies change of the nutrient concentration.

However, there are some other reasons for which the bloom skips. For example, the toxic chemicals released by the TPP change over time [28, 35], and this may be another reason for the bloom to skip. In view of this experimental observation, we modify the model (4) with a periodic function of θ. First, assuming that there is no modulation in the growth rate of the phytoplankton population due to seasonal environmental conditions, to obtain

$$\left.\begin{aligned} \frac{dN}{dt} &= a - bNP - eN \\ \frac{dP}{dt} &= cNP - dP - \frac{\theta(t)P^2}{\mu^2 + P^2}. \end{aligned}\right\} \tag{11}$$

In (11), we suppose that there is a variation in the production of toxic chemicals released by TPP populations so that, in some periods of the year, toxic chemicals are higher than in

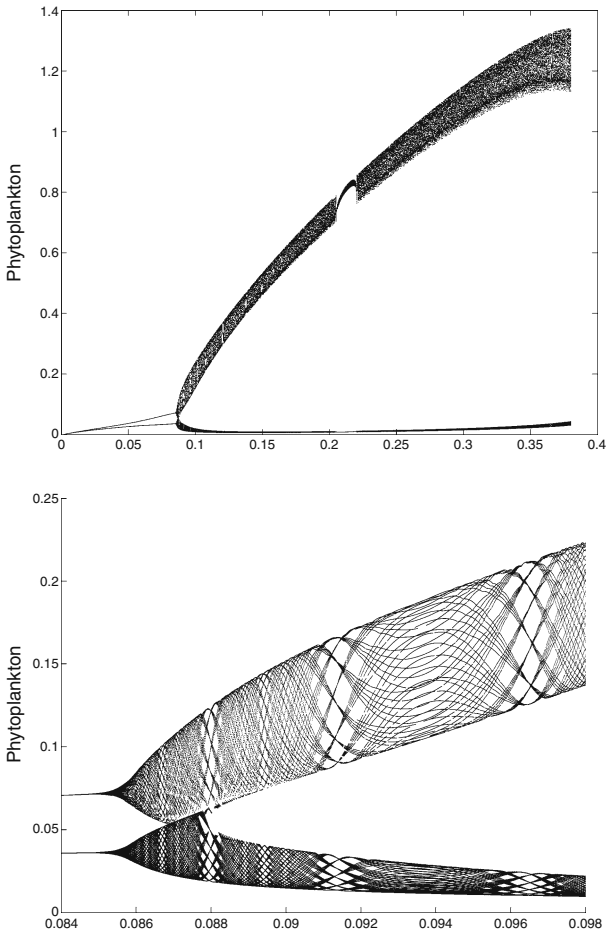

Fig. 5 Bifurcation diagram of equation (11). *Top* Phytoplankton population is plotted as a function of constant inflow rate a. The *bottom image* shows the detail of the *top image* for the range [0.086, 0.098]

other periods. The rate of toxin release θ by TPP can, thus, be represented by the following periodic function:

$$\theta(t) = \lambda\,(1 - \delta\sin(\omega t))$$

where $0 < \delta < 1$ controls the strength of the forcing.

Now, we state some results on the model (11). The proofs and certain technical lemmas are deferred to the Appendix.

Lemma 3 *Solutions of* (11) *are bounded and remain in the positive octant.*

The next theorem provides a sufficient condition for which the phytoplankton population goes to extinction.

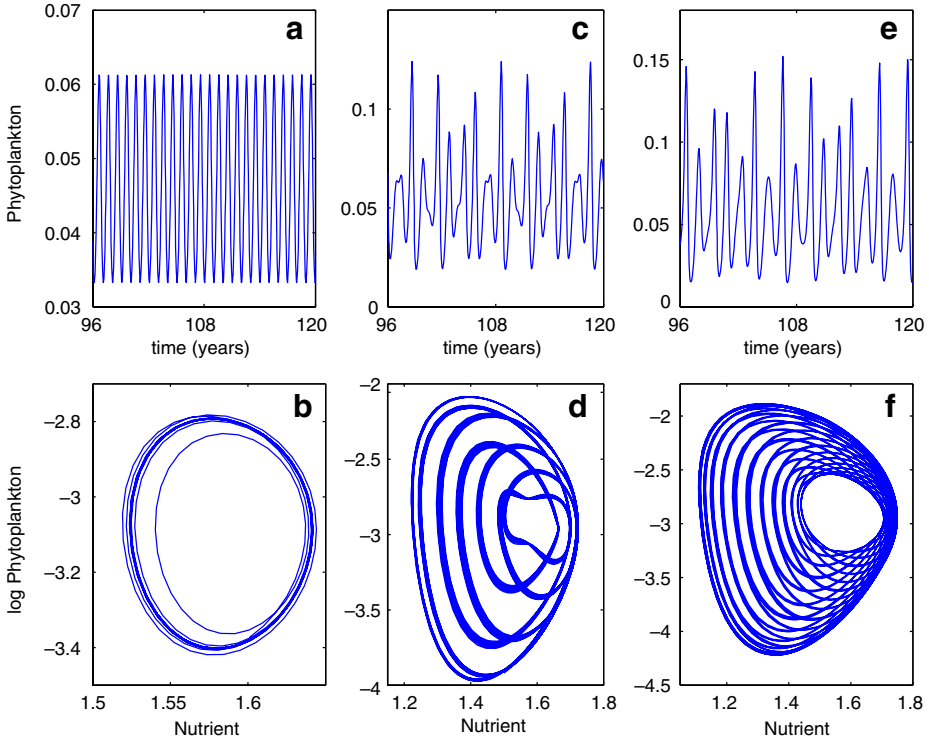

Fig. 6 Chaotic solutions of the forced model (11). **a**, **b** ($a = 0.075$) Limit cycle with annual bloom. **c**, **d** ($a = 0.088$) Quasi-period with bloom maxima changing in amplitude every year. **e**, **f** ($a = 0.09$) Chaotic oscillation. Fixed parameters: $b = 1$; $c = 1$; $d = 1$; $e = 0.0012$; $\omega = 0.19$; $\delta = 0.1$; $\mu = 0.05$. Compare the differences with the bifurcation diagram Fig. 8 for the three values of a chosen here, $a = 0.075,\ 0.088,\ 0.09$

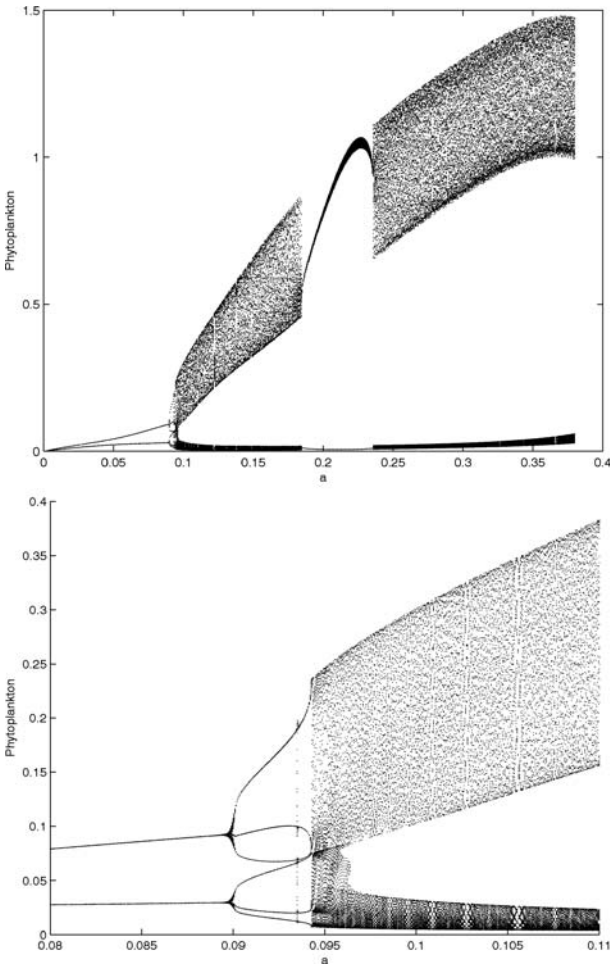

Fig. 7 Bifurcation diagram of equation (12). *Top*: Phytoplankton population plotted as a function of constant inflow rate a. The *bottom image* shows detail of the *top image* for the range [0.08–0.11]

Theorem 2 *A sufficient condition for* $\lim_{t\to\infty} P(t) = 0$ *and* $\lim_{t\to\infty} N(t) = \frac{a}{e} + o(1)$ *is* $ac - de < 0$.

Numerical experiments of system (11) have been performed to observe the seasonal bloom and skipping dynamics of the nutrient–phytoplankton model. The inclusion of periodicity in the toxic chemicals results in annual limit cycle behaviour (Fig. 4a, b). If we increase the value of constant inflow, the periodic oscillation of one cycle changes to periodic oscillation of period two which is clear from Fig. 4c and d. Further increase in nutrient inflow gives a different limit cycle of period 2. However, we observe that blooms occur every year and a major bloom is always followed by a very small bloom. From Fig. 4e and f, we can visualise this skipping phenomena of phytoplankton bloom. It is to be noted that, during the time of skipping, the nutrient level still continues to increase (Fig. 4f), which results in the increase of bloom height.

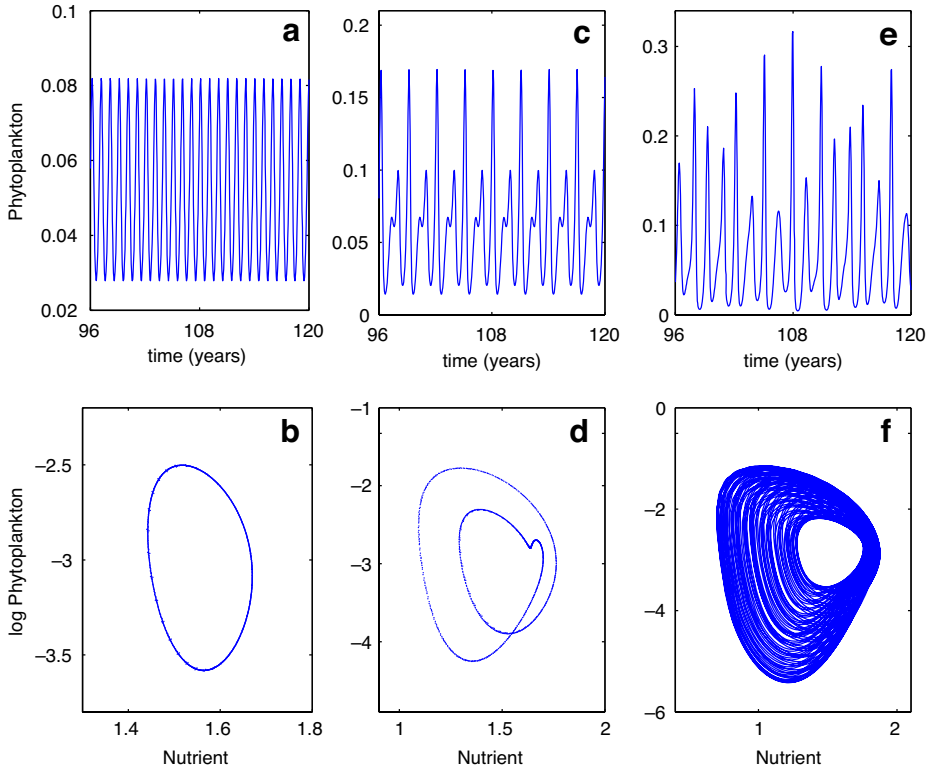

Fig. 8 Chaotic solutions of the forced model (12). **a**, **b** ($a = 0.082$) Limit cycle with annual bloom. **c**, **d** ($a = 0.0925$) Periodic-doubled orbit. **e**, **f** ($a = 0.102$) Chaotic oscillation. Fixed parameters are the same as in Fig. 6

3.1 Some more Interesting Behaviours

The complex dynamics of our proposed model (11) from limit-cycles to chaos are described in the bifurcation diagram of Fig. 5, where we plot the phytoplankton population as a function of the constant inflow rate a. The behaviour of (11) is very complicated, including many chaotic bands, periodic windows and crises, i.e., the phenomena for which the chaotic attractor can suddenly appear or disappear or change size discontinuously as a parameter smoothly varies [36].

From the bifurcation diagram shown in Fig. 5a, when a is very low, below 0.025, a stable focus is observed. When the parameter a is increased beyond 0.025, we observe a limit cycle periodic oscillation for ($a \in A \equiv [0.025, 0.085]$) implying periodic bloom, also illustrated in Fig. 6a–b. As the value of a is further increased, we observe two-piece chaos. Unlike the common period-doubling route to chaos, here, we observe the frequent occurrence of chaos followed by sudden changes of attractor (crisis) in the range of [0.086–0.098]; see Fig. 6c, d. For example, when $a = 0.088$ the system shows a period 6-cycle, while for some lower values, it exhibits chaotic oscillations. Then, it again enters into the chaotic region. When the value of a is increased to 0.0915, the system again shows period 5-cycle oscillations. For further increase in the value of a, the system goes through high period cyclic oscillations,

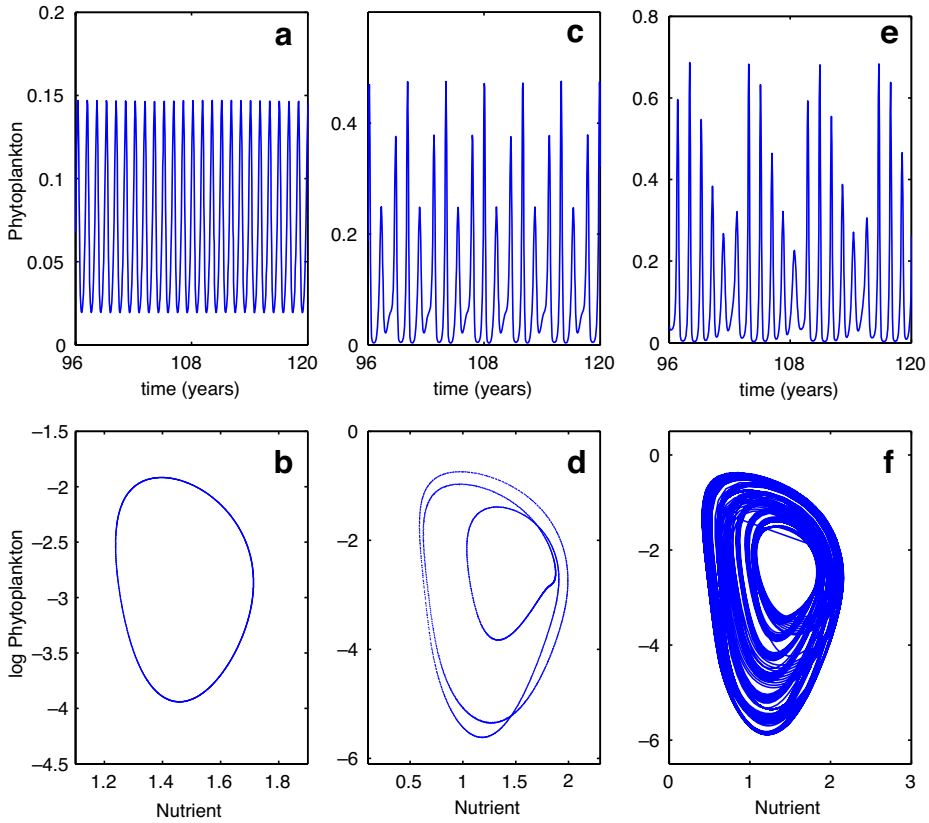

Fig. 9 Chaotic solutions of the forced model (12) with $T = 10$. **a**, **b** ($a = 0.102$) Limit cycle with annual bloom. **c**, **d** ($a = 0.125$) Period three. **e**, **f** ($a = 0.15$) Chaotic oscillation. Fixed parameters are the same as Fig. 6

Fig. 6e, f. The bifurcation diagram of Fig. 5 and the phase plane and time series plots shown in Fig. 6 should be compared by identifying the values of the parameter a leading to Fig. 6 with the corresponding behaviour of the bifurcation diagram of Fig. 5.

Finally, we consider both the effect of seasonal modulation of the phytoplankton growth $\beta(t)$ and the variation in the rate of toxin production $\theta(t)$. Under this assumption, system (4) becomes

$$\left.\begin{aligned} \frac{dN}{dt} &= a - b\beta(t)NP - eN \\ \frac{dP}{dt} &= c\beta(t)NP - dP - \frac{\theta(t)P^2}{\mu^2 + P^2}. \end{aligned}\right\} \tag{12}$$

The corresponding bifurcation diagram with phytoplankton population plotted as a function of the constant inflow rate a is given in Fig. 7. Comparing it with the one given in Fig. 5, we observe that the system (12) enters into the chaotic region for $a = 0.086$, while

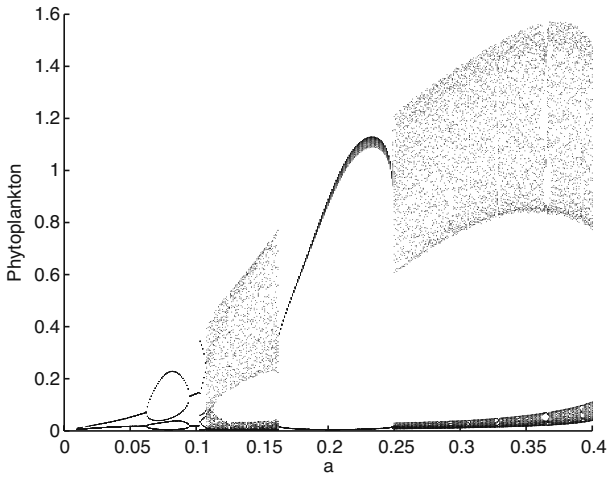

Fig. 10 Bifurcation diagram of equation (12) with $T = 10$, with a possible phase shift. Phytoplankton population is plotted as a function of constant inflow rate a

the system (11) enters it for $a = 0.094$. Figures 7 and 8 shows the system (12) to enter the chaotic region following the common period doubling route to chaos, and does not exhibit significant changes of attractor (crisis), both features being in contrast to what happens in Figs. 5 and 6 for (11).

Next, we consider a possible phase shift in the two forcing terms. Without changing the form $\beta(t)$, we take $\theta(t)$ in (12) as follows:

$$\theta(t) = \lambda\,(1 - \delta \sin(\omega(t - T))).$$

Taking $T = 10$, i.e. almost phase opposition, we observe the same dynamical behaviour of the system, but for different values of a as shown in Figs. 9 and 10. This is more clear if we compare the bifurcation diagram given in Fig. 7 with the one given in Fig. 10, which gives the bifurcation diagram corresponding to Fig. 9, with phytoplankton population plotted as function of the constant inflow rate a.

Comparing these two bifurcation diagrams, we observe that the basic structures of both Figs. 7 and 10 are the same but there is a difference in the range of a. Similar results hold for intermediate values of T.

4 Conclusion

Huppert et al. [11] developed one of the first successful nutrient–phytoplankton interaction models to describe the planktonic bloom phenomenon. Despite its simplicity, the model provides fascinating insights into many of the events occurring in different lakes and oceans. It demonstrates that the nutrient–phytoplankton dynamics may be governed by a generic threshold effect, i.e. a critical buildup of nutrients is required before a phytoplankton bloom can be triggered. An extension of the study investigates a suite of oscillatory, excitable, and chaotic bottom-up phytoplankton–nutrient models to understand the more complicated temporal dynamics seen in empirical data such as those of the river Danube and Lake Kinneret, as described in Huppert et al. [13]. However, there are two drawbacks to in this approach. The unforced model (1) is unable to generate periodic cycles and is,

thus, unsuitable for modeling seasonally recurring outbreaks. Secondly, the effect of toxic chemicals released by the TPP population has been neglected.

In our present study, we have considered the effect of nutrient concentration on the growth rate of the phytoplankton population in the presence of toxins. From our numerical simulations, we observe that the results obtained by Huppert et al. [11] hold when the rate of toxin release θ is under a certain critical value θ_c, see Fig. 1a. If θ becomes greater than θ_c, as in the case of Fig. 1b and c, we observe different dynamical behaviours. It is interesting to note that, for a certain range of θ, the model exhibits periodic solutions (see Fig. 1b). We also observe that toxin produced by the TPP may act as a biological control in the termination of the planktonic bloom (see Fig. 1c), which is in good agreement with some earlier findings. We also observe that the nutrient recycling increases the chance of recurring blooms; see Fig. 6.

Huppert et al. [13] have shown that the modulation in the growth rate of the phytoplankton population due to seasonal environmental conditions is the main reason for the skipping phenomenon and the occurrence of chaotic behaviour in the phytoplankton population. Here, we have shown that the variation in the rate of toxin release by the TPP plays an equally important role for the occurrence of the above phenomena; see Figs. 7 and 8. Moreover, from Fig. 8, we observe that our model equation (12) has the potential to show different complicated dynamical behaviours like chaotic bands, periodic windows and crises.

We have already mentioned that Chattopadhyay and his co-workers, combining field observations and mathematical models, established that toxic chemicals may act as a biocontrol for the termination of plankton blooms [16, 21]. Those studies were mainly based on a phytoplankton–zooplankton model or nutrient–phytoplankton–zooplankton model. In this paper, we have studied the role of toxic chemicals released by the TPP population in a nutrient–phytoplankton population, where the zooplankton population is absent. We thus conclude that the effect of toxic chemicals released by TPP cannot even be ignored in bottom-up models.

Acknowledgements The authors gratefully acknowledge the comments of the referees and of the editor on the previous version of the paper. The comments have immensely improved the content and the presentation of the manuscript.

Appendix

Proof of Lemma 3 Since $N(0) > 0$, from the representation

$$N(t) = N(0)\left\{\exp\left(-\int_0^t (bP(t)+e)dt\right)\right\} + a\int_0^t \exp\left(-\int_\xi^t (bP(\mu)+e)d\mu\right)d\xi,$$

we have $N(t) > 0$ for all t.

Suppose $P(t)$ is not positive for all $t \geq 0$. Because $P(0) > 0$, there exists a point T_0 with $P(T_0) = 0$ and $P(t) > 0$ for $0 \leq t \leq T_0$. For $0 \leq t \leq T_0$,

$$\frac{P'(t)}{P(t)} > cN(t) - d - \lambda(1+\delta)\frac{P(t)}{\mu^2 + P^2(\xi)}$$

or,

$$\frac{P'(t)}{P(t)} > -d - \lambda(1+\delta)\frac{P(t)}{\mu^2 + P^2(\xi)}.$$

Integrating from 0 to T_0 and taking the exponentials of both sides, it follows that

$$P(T_0) \geq P(0) \exp \int_0^{T_0} \left(-d - \lambda(1+\delta) \frac{P(t)}{\mu^2 + P^2(\xi)} \right) d\xi > 0.$$

This is a contradiction, and hence, $N(t)$ and $P(t)$ are positive for all $t \geq 0$. Multiplying the equations for P in (11) by $\frac{b}{c}$ and adding yields

$$N'(t) + \frac{b}{c} P'(t) = a - eN(t) - \frac{db}{c} P(t) - \frac{b}{c} \lambda(1 - \delta \sin \omega t) \frac{P(t)^2}{\mu^2 + P(t)^2}.$$

Let $\eta = \min\{e, d\}$ and $F(t) = \frac{b}{c} \lambda(1 - \delta \sin \omega t) \frac{P(t)^2}{\mu^2 + P(t)^2}$. Then,

$$N'(t) + \frac{b}{c} P'(t) \leq a - \eta \left(N(t) + \frac{b}{c} P(t) \right) - F(t).$$

Comparing the solutions $N'(t) + \frac{b}{c} P'(t)$ of the above inequality with the solutions of

$$z'(t) = a - \eta z(t) - F(t)$$

$$z(0) = N'(0) + \frac{b}{c} P'(0)$$

it follows that

$$N(t) \leq z(t) \text{ for all } t \geq 0,$$

or,

$$N'(t) + \frac{b}{c} P'(t) \leq \left(z(0) - \frac{a}{\eta} \right) \exp(-\eta t) + \frac{a}{\eta} - \int_0^t \exp\{-\eta(t-\xi)\} F(\xi) d\xi.$$

Suppose first, $\int_0^t \exp(\eta\xi) F(\xi) d\xi < \infty$. Then,

$$\lim_{t \to \infty} \int_0^t \exp\{-\eta(t-\xi)\} F(\xi) d\xi = 0.$$

If

$$\int_0^t \exp(\eta\xi) F(\xi) d\xi = \infty,$$

then L'Hôspital's rule yields

$$\begin{aligned} \lim_{t \to \infty} \int_0^t \exp\{-\eta(t-\xi)\} F(\xi) d\xi &= \lim_{t \to \infty} \frac{\int_0^t \exp(\eta\xi) F(\xi) d\xi}{\exp(\eta t)} \\ &= \lim_{t \to \infty} \frac{\exp(\eta t) F(t)}{\eta \exp(\eta t)} = \frac{1}{\eta} \lim_{t \to \infty} F(t). \end{aligned}$$

Because $F(t)$ is bounded and $\lim_{t \to \infty} \left(z(0) - \frac{a}{\eta} \right) \exp(-\eta t)$, the sum on the left side is bounded, and because each term is positive, each term is bounded.

The main result is proven by means of the following lemmas. □

Lemma 4 *Let $N(t)$, $P(t)$ be solutions of (11). Then,*

$$N(t) = A \exp(-et) + \frac{a}{e} + \frac{b}{c} h(t) \tag{13}$$

where $A = N(0) + \frac{b}{c}P(0) - \frac{a}{e}$,

$$h(t) = \int_0^t F_1(\xi)\exp\{-e(t-\xi)\}d\xi \; - P(t), \tag{14}$$

and $F_1(\xi) = (e-d)P(\xi) - \lambda(1-\delta\sin\omega t)\frac{P(\xi)^2}{\mu^2+P(\xi)^2}$.

Proof We have

$$N'(t) + eN(t) = a - bN(t)P(t),$$

or,

$$N(t) = \exp\left\{N(0) + a\int_0^t \exp(e\xi)d\xi - b\int_0^t N(\xi)P(\xi)\exp(e\xi)d\xi\right\}.$$

Then, (13) follows after an integration. □

Lemma 5 *If* $\lim_{t\to\infty} P(t) = 0$, *then* $\lim_{t\to\infty} h(t) = 0$.

Proof Suppose first, $\int_0^\infty F_1(\xi)\exp(e\xi)d\xi < \infty$. Then, $\lim_{t\to\infty}\int_0^\infty F_1(\xi)\exp\{-e(t-\xi)\}d\xi = 0$. Hence, $\lim_{t\to\infty} h(t) = 0$. If

$$\int_0^\infty F_1(\xi)\exp(e\xi)d\xi = \infty$$

then L'Hôspital's rule yields

$$\begin{aligned}\lim_{t\to\infty}\int_0^t \exp\{-\eta(t-\xi)\}F_1(\xi)d\xi &= \lim_{t\to\infty}\frac{\int_0^t \exp(\eta\xi)F_1(\xi)d\xi}{\exp(\eta t)}\\ &= \lim_{t\to\infty}\frac{\exp(\eta t)F_1(t)}{\eta\exp(\eta t)} = \frac{1}{\eta}\lim_{t\to\infty} F_1(t) = 0.\end{aligned}$$

Hence, $\lim_{t\to\infty} h(t) = 0$. □

Lemma 6 *If* $\lim_{t\to\infty} P(t) = 0$, *then* $ac - de < 0$.

Proof From the assumption and Lemma 5, it follows that $\lim_{t\to\infty} P(t) = 0$. By the representation (13), we have $N(t) = \frac{a}{e} + 0(1)$. For a given $\epsilon > 0$, there exists $t_0 > 0$ such that $\frac{a}{e} - \epsilon < N(t) < \frac{a}{e} + \epsilon$, for $t \geq t_0$. We have, for $t \geq t_0$,

$$\begin{aligned}P'(t) &= -\lambda(1-\delta\sin\omega t)\frac{P(t)^2}{\mu^2+P(t)^2} + (cN(t)-d)P(t)\\ &\geq -\lambda(1-\delta\sin\omega t) + (cN(t)-d)P(t)\\ &> -\lambda(1-\delta\sin\omega t) + \left(c\left(\frac{a}{e}-\epsilon\right)-d\right)P(t)\end{aligned}$$

or,

$$P'(t) > -\lambda(1-\delta\sin\omega t) + MP(t)$$

where

$$M = \left(c\left(\frac{a}{e}-\epsilon\right)-d\right).$$

Comparing the solutions $P(t)$ of the above inequality with solutions of

$$z'(t) = -\lambda(1 - \delta \sin \omega t) + Mz(t)$$
$$z(0) = P(0)$$

it follows that

$$P(t) > \left[P(0) - \lambda \int_0^t (1 - \delta \sin \omega \xi) \exp(-M\xi) d\xi \right] \exp(Mt).$$

or,

$$P(t) > \left[P(0) - \frac{\lambda}{M} - \frac{\lambda M \omega}{M^2 + \omega^2} \right] \exp(Mt) + \lambda \left[\frac{1}{M} - \frac{M}{\sqrt{M^2 + \omega^2}} \sin\left(\omega t - \tan^{-1} \frac{\omega}{M} \right) \right]$$

i.e.

$$P(t) > \left[P(0) - \frac{\lambda}{M} - \frac{\lambda M \omega}{M^2 + \omega^2} \right] \exp(Mt) + \lambda \left[\frac{1}{M} - 1 \right].$$

Taking the limit as $t \to \infty$ on both sides and using the assumption $\lim_{t \to \infty} P(t) = 0$, the above inequality holds only if $M = c(\frac{a}{e} - \epsilon) - d) < 0$. Because ϵ is arbitrarily small and M is independent of t_0, it follows that $ac - de < 0$. □

Proof of Theorem 2 Theorem 2 follows directly from Lemma 4, Lemma 5 and Lemma 6. □

References

1. Hay, M.E., Kubanek, J.: Community and ecosystem levels consequences of chemical cues in lankton. J. Chem. Ecol. **28**, 2001–2016 (2002)
2. Anderson, D.M., Kaoru, Y., White, A.W.: Estimated Annual Economic Impacts from Harmful Algal Blooms (HABs) in the United States Sea Grant Woods Hole. NCCOS, Silver Spring (2000)
3. Clother, D.R., Brindley, J.: Excitability of an age-structured plankton ecosystem. J. Math. Biol. **39**, 377–420 (1999)
4. Edwards, A.M., Brindley, J.: Oscillatory behaviour in a three-component plankton population model. Dyn. Stab. Syst. **11**, 347–370 (1996)
5. Edwards, A.M., Brindley, J.: Zooplankton mortality and the dynamical behaviour of plankton population models. Bull. Math. Biol. **61**, 303–339 (1999)
6. Pitchford, J.W.: Dynamics of multi-species plankton population. Ph.D. thesis, University of Leeds (1997)
7. Pitchford, J.W., Brindley, J.: Iron limitation, grazing pressure and oceanic high nutrient-low chorophyll (HNLC) regions. J. Plankton Res. **21**, 525–547 (1999)
8. Truscott, J.E., Brindley, J.: Equilibria, stability and excitability in a general-class of plankton population-models. Philos. Trans. R. Soc. Lond. Ser. A Math. Phys. Sci. **347**, 703–718 (1994)
9. Truscott, J.E., Brindley, J.: Ocean plankton populations as excitable media. Bull. Math. Biol. **56**, 981–998 (1994)
10. Chan, T.U., Robson, B.J., Hamilton, D.P.: Modelling phytoplankton succession and biomass in seasonal West Australian estuary. Verh. Int. Ver. Limnol. **28**(2), 1086–1088 (2003)
11. Huppert, A., Blasius, B., Stone, L.: A model of phytoplankton blooms. Am. Nat. **159**, 156–171 (2002)
12. Huppert, A., Olinky, R., Stone, L.: Bottom-up excitable models of phytoplankton blooms. Bull. Math. Biol. **66**, 865–878 (2004)
13. Huppert, A., Blasius, B., Olinkya, R., Stonea, L.: A model for seasonal phytoplankton blooms. J. Theor. Biol. **236**, 276–290 (2005)
14. Robson, B.J., Hamilton, D.P.: Three-dimensional modelling of a Microcystis bloom event in the Swan River estuary. Ecol. Model. **174**(1–2), 203–222 (2004)
15. Segal, R., Waite, A.M., Hamilton, D.P.: Transition from planktonic to benthic algal dominance along a salinity gradient. Hydrobiologia **556**, 119–135 (2006)

16. Chattopadhyay, J., Sarkar, R.R., Mandal, S.: Toxin-producing plankton may act as a biological control for planktonic blooms field study and mathematical modelling. J. Theor. Biol. **215**, 333–344 (2002)
17. Chattopadhyay, J., Sarkar, R.R., el Abdllaoui, A.: A delay differential equation model on harmful algal blooms in the presence of toxic substances. IMA J. Math. Appl. Med. Biol. **19**, 137–161 (2002)
18. Chattopadhyay, J., Sarkar, R.R., Pal, S.: Mathematical modelling of harmful algal blooms supported by experimental findings. Ecol. Complex. **1**, 225–235 (2004)
19. Pal, S., Chatterjee, S., Chattopadhyay, J.: Role of toxin and nutrient for the occurence and termination of plankton bloom - results drawn from field observations and a mathematical model. Biosystems **90**(1), 87–100 (2007)
20. Roy, S., Alam, S., Chattopadhyay, J.: Competing effects of toxin-producing phytoplankton on overall plankton populations in the Bay of Bengal. Bull. Math. Biol. **68**, 2303–2320 (2006).
21. Sarkar, R.R., Chattopadhyay, J.: Occurence of planktonic blooms under environmental fluctuations and its possible control mechanism—mathematical models and experimental observations. J. Theor. Biol. **224**, 501–516 (2003)
22. Sarkar, R.R., Pal, S., Chattopadhyay, J.: Role of two toxin-producing plankton and their effect on phytoplankton-zooplankton system—a mathematical study supported by experimental findings. Biosystems **80**, 11–23 (2005)
23. Hallam, T., Clark, C., Jordan, G.: Effects of toxicants on populations: a qualitative approach. II. First order kinetics. J. Theor. Biol. **18**, 25–37 (1983)
24. Shilo, M.: Formation and mode of action of algal toxins. Bacteriol. Rev. **31**, 180–193 (1967)
25. Dafni, Z., Ulitzur, S., Shilo, M.: Influence of light and phosphate on toxin production and growth of Prymnesium parvum. J. Gen. Microbiol. **70**, 199–207 (1972)
26. Pan, Y., Subba Rao, D.V., Mann, K.H.: Changes in domoic acid production and cellular chemical composition of the toxigenic diatom Pseudonitzschia multiseries under phosphate limitation. J. Phycol. **32**, 371–381 (1996)
27. Sohet, K., Pereira, A., Braeckman, J.C., Houvenaghel, G.: Growth and toxicity of Prorocentrum lima (Ehrenberg) dodge in different culture media: effects of humic acids and organic phosphorus. In: Lassus, P., Arzul, G., Erard-le Denn, E., Gentien, P., Marcaiillou-Le Baut, C. (Eds.), Harmful Marine Algal Blooms. Lavoisier Intercept, New York, pp. 669–674 (1995)
28. Graneli, E., Johansson, N.: Effects of the toxic haptophyte Prymnesium parvum on the survival and feeding of a ciliate: the influence of different nutrient conditions. Mar. Ecol. Prog. Ser. **254**, 49–56 (2003)
29. Keating, K.I.: Blue-green algal inhibition of diatom growth: transition from mesotrophic to eutrophic community structure. Science **199**, 971–973 (1978)
30. Keating, K.I.: Allelopathic influence on blue-green bloom sequence in a eutrophic lake. Science **196**, 885–887 (1977)
31. Schmidt, L.E., Hansen, P.J.: Allelopathy in the prymnesiophyte Chyrsochromulina polylepis: effect of cell concentration, growth phase and pH. Mar. Ecol. Prog. Ser. **216**, 67–81 (2001)
32. Windust, A.J., Wright, J.L.C., McLachlan, J.L.: The effects of the diarrhetic shellfish poisoning toxins okadaic acid and dinophysistoxin-1, on the growth of microalgae. Mar. Biol. **126**,
33. Nagumo, M.: Über die Lage der Integralkurven gewönlicher Differentialgleichungen. Proc. Phys. Math. Soc. Jpn. **24**, 551 (1942)
34. Turner, J.T., Tester, P.A.: Toxic marine phytoplankton, zooplankton, grazers, and pelagic food webs. Limnol. Oceanogr. **4205**(2), 1203–1214 (1997) 19–25 (1996)
35. Johansson, N., Graneli, E.: Influence of different nutrient conditions on cell density, chemical composition and toxicity of Prymnesium parvum (Haptophyta) in semi-continuous cultures. J. Exp. Mar. Biol. Ecol. **239**, 243–258 (1999)
36. Tang, S.Y., Chen, L.S.: Chaos in functional response host-parasitoid ecosystem models. Chaos Solitons Fractals **13**, 875–884 (2002)